Spatial prediction of leaf chlorophyll content in cotton crop using drone-derived spectral indices

P. Shanmugapriya[1,*], K. R. Latha[1], S. Pazhanivelan[2], R. Kumaraperumal[3], G. Karthikeyan[4] and N. S. Sudarmanian[5]

[1]Department of Agronomy, [2]Water Technology Centre, [3]Department of Remote Sensing and GIS, and
[4]Department of Plant Pathology, Tamil Nadu Agricultural University, Coimbatore 641 003, India
[5]Krishi Vigyan Kendra, Aruppukottai 626 107, India

Crop health monitoring and assessment have become more successful with the advent of remote sensing technology in agriculture. Using this technology, retrieving information about crop biophysical parameters on a non-destructive basis at spatial and temporal scales has been made possible. Several drone-derived spectral vegetation indices (VIs) have assessed crop growth status in a larger farming area. In this study, we generated VI maps for a cotton field area in the Tamil Nadu Agricultural University, Coimbatore, India. The ground-truth chlorophyll data (SPAD-502 Minolta meter) were collected from the field on the same day of drone image acquisition. Pearson correlation analysis and regression analysis were done for validation and accuracy of the ground-truth chlorophyll data and VIs. The study reveals that obtaining near real-time chlorophyll content using high spatial resolution drone images is quick and reliable.

Keywords: Chlorophyll content, cotton crop, drone, multispectral images, spectral indices.

THE advancement of remote sensing technology in agriculture has made it possible to acquire information at spatial and temporal scales. Drone (dynamic remotely operated navigation equipment), commonly known as unmanned aerial vehicle (UAV), has been primarily developed for civilian and military purposes[1]. It could be an inexpensive and more practical replacement for satellite remote sensing in agriculture for monitoring vegetation status[2]. Nowadays, a drone equipped with multispectral sensors can be used to assess the in-field spatial variability of crop conditions. The modern multispectral sensors have made remote sensing more informative and expanded its range of applications[3]. It is a valuable tool for assessing crop condition, monitoring vegetation cover, nutrient and water status, crop quality, i.e. infestations, weed/pest/disease, crop yield and production forecasting, etc.[4].

*For correspondence. (e-mail: shanmugapriyapalanisamy96@gmail.com)

The agricultural remote sensing users apply numerous spectral vegetation indices (VIs) of nominal reflectance values derived from different multispectral bands of the following wavelengths: blue (440–510 nm), green (520–590 nm), red (630–685 nm), red edge (690–730 nm) and near-infrared (760–850 nm) for intuitive visualization of crop growth status[5]. Indices are defined as the ratio of the difference between the reflectance of different spectral bands, which provide different data layers[6]. The indices help monitor crop growth status as they can enhance the spectral differences at specific wavelengths[7]. VI is a data-processing method that considers the vegetation spectrum information using different linear combinations of the ratio between the visible and near-infrared spectrum[8]. The fundamental reason for this is that plant has a high sensitivity to visible and near-infrared wavelengths, and a combination of these two bands is effective. VIs strengthen the information about closed vegetation.

Chlorophyll is a good predictor of plant vigour and health, allowing for the estimation of final crop yield. The chlorophyll content indirectly relates to the crop nitrogen status, ultimately deciding the crop productivity. However, the manual method of measuring chlorophyll content is destructive and time-consuming, and obtaining information on spatial context is inaccurate. Images from a sensor mounted on a portable UAV will be further useful to understand image-based crop biomass and nitrogen content estimations[9]. Chlorophyll-specific VIs, in particular, have proven to be more relevant than normalized VIs in some circumstances, as they encompass a variety of combinations from bands that reflect vegetation accurately[10]. These VIs were selected to reflect band combination variations and sensitivity to soil background, biomass and chlorophyll content[11]. Chlorophyll has strong red absorption peaks and prominent near-infrared reflectance peaks[12]. Red absorption is at its highest between 660 and 680 nm. This is because, except for high chlorophyll content, the 660–680 nm absorption range tends to be saturated at low chlorophyll levels and to reflect in the near-infrared region, decreasing the sensitivity of the spectral indices based on this wavelength[13]. The goal is to detect subtle changes in nitrogen content/deficiencies[14].

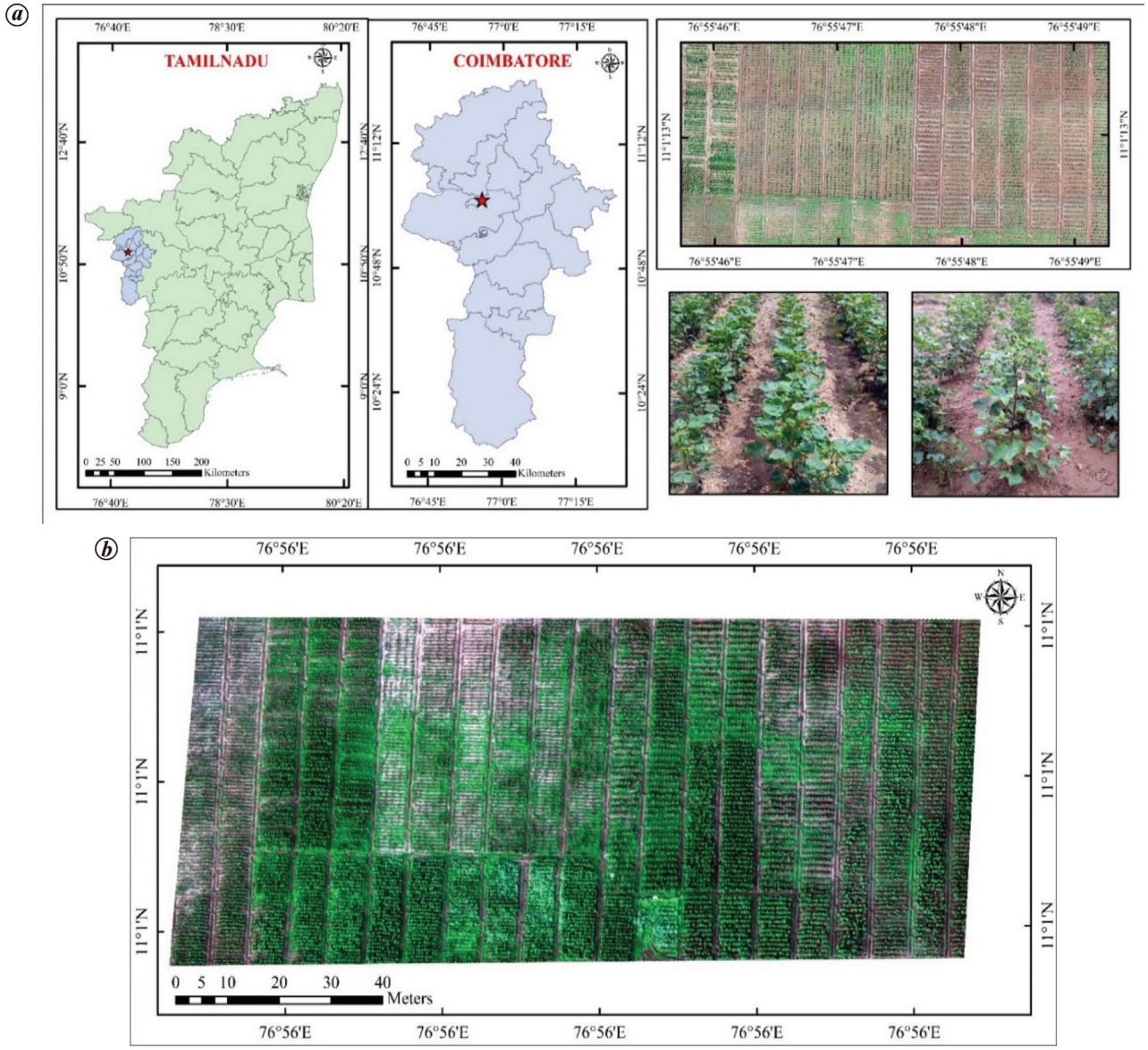

Figure 1. ***a***, Location of the study area. ***b***, Aerial view of the field.

In precision agriculture, for a variable rate of fertilizer applications, data obtained at different spatial levels will be more beneficial for successful decision-making. This study aimed to (i) estimate cotton chlorophyll content at the spatial level using drone-derived multispectral VIs and (ii) validate the derived spectral indices using chlorophyll data measured using a SPAD meter.

Materials and methods

Study area

The experiment was carried out in a cotton research field at the Department of Cotton, Tamil Nadu Agricultural University, Coimbatore, India. The study area covers about 3.5 acres with geo-coordinates from 11°01′13.99″N lat. and 76°55′44.69″E long. to 11°01′11.98″N lat. and 76°55′49.82″E long. at an altitude of 429 m amsl (Figure 1).

Data collection

Image acquisition: This study used a quadcopter drone with a payload of Micasense RedEdge multispectral cameras (Table 1). The significant advantage of this equipment is its vertical take-off and landing capabilities, which can be operated from confined places. Furthermore, this aircraft can be automated by giving waypoints. Ground control station software (UgCS) was used to plan the flight path (waypoints, altitude, heading direction and speed). UgCS Mapper is a lightweight photogrammetry software that can work

purely offline in the field, create maps and elevation data on the fly and stitch multispectral images into orthomosaics.

A flight mission (Figure 2) was carried out on 22 December 2021, under a clear sky between 11 am and 12 pm for 9 min for multispectral image collection. The camera captures the photograph, stores it in memory and sends it to the ground station through telemetry. In addition, MicaSense RedEdge calibration was done using a calibrated reflectance panel (CRP). The calibration was done immediately before each flight according to the instructions given in the calibration manual.

Ground data collection: The ground data were collected on 22 December 2021, when drone images were captured. Non-destructive chlorophyll readings were measured using the SPAD-502 Minolta meter as the light transmittance ratio at a wavelength of 650 and 940 nm at three points of the third leaf and averaged to get the precise result. Fifteen geo-tagged ground data were collected randomly to validate VI.

Data processing

Image processing: Multispectral images obtained were processed (Figure 3) using Pix4D mapper software. The raw data were processed, analysed and geo-referenced to produce an orthomosaic. In addition, multiple overlapped images obtained were stitched together to generate a large map for an accurate geo-referenced map.

Vegetation index processing: VIs are the primary tool for analysing aerial images[15]. First, post-processed photographs were used to generate VIs maps using ArcGIS 10.6 software. Then, the VI formula (Table 2) was applied to obtain information from the processed data. The most common VI is NDVI, which plays a significant role in assessing crop growth status, vigour and yield. However, some of the red edge-based vegetation indices, viz. normalized difference red edge index (NDRE), red edge difference vegetation index (REDVI) and modified chlorophyll absorption ratio index (MCARI) perform better when compared to NDVI[16]. In addition, the green normalized difference vegetation index (GNDVI) and optimized soil adjusted vegetation index (OSAVI) help predict the chlorophyll content of the vegetation. Utilizing the ground data coordinates, spectral information from the different VIs was extracted using the pixel-by-value tool in ArcGIS 10.6. Finally, the extracted spectral information was subjected to statistical analysis (Figures 2 and 3).

Data acquisition

Step 1: UAV-mounted with a multispectral sensor was used to collect aerial images of cotton crops and geo-tagged ground-truth data were collected using the SPAD meter.

Data processing

Step 2: Initial processing was done using Pix4D software.

Step 3: Next, point cloud and mesh were generated.

Step 4: Digital surface models, digital terrain models, orthomosaics and indices were calculated.

Step 5: VIs were estimated using the raster calculator tool in Arc10.6.

Table 1. Unmanned aerial vehicle flight information and sensor specifications

Platform	Quadcopter
Flight speed (m s^{-1})	8
Flight altitude (m)	30
Per cent overlap	70
Ground sample distance	8 cm per pixel (per band)
Sensor model	Micasense RedEdge
Spectral bands	Blue, green, red, red edge, near-IR
Wavelength (nm)	Blue (475 nm centre, 20 nm bandwidth), green (560 nm centre, 20 nm bandwidth), red (668 nm centre, 10 nm bandwidth), red edge (717 nm centre, 10 nm bandwidth) and near-IR (840 nm centre, 40 nm bandwidth)
Sensor size (mm)	23.5 × 15.6
Image resolution (pixels)	10,116 × 4,219

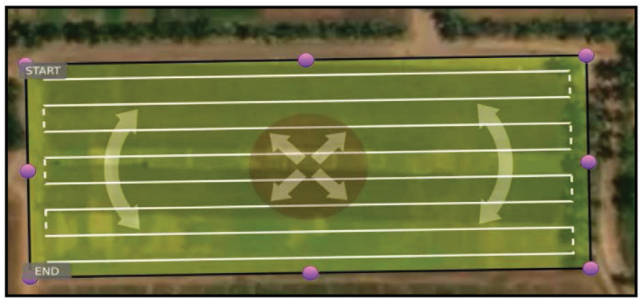

Figure 2. Unmanned aerial view route plan of the study area.

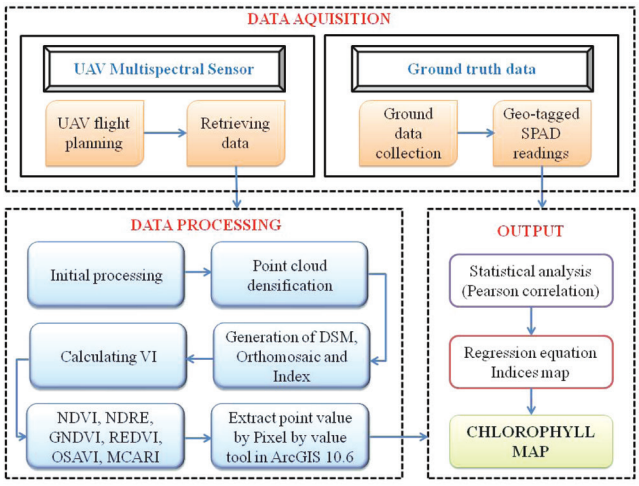

Figure 3. Flow chart depicting the methodology used.

Table 2. Vegetation indices used in the study

Index	Equation	Applications
NDVI	$\frac{NIR - R}{NIR + R}$	To estimate vegetation growth and biomass quantitatively[25].
NDRE	$\frac{NIR - RE}{NIR + RE}$	It is a much better indicator for crop health/vigour and is also used for N management in crops[26].
GNDVI	$\frac{NIR - G}{NIR + G}$	It is one of the most widely used vegetation indices for estimating nitrogen uptake in the crop canopy and chlorophyll content[27].
REDVI	NIR – RE	It is mainly used for estimating the N-uptake and concentration[28].
OSAVI	$\frac{1.16\,(NIR - R)}{NIR + R + 0.16}$	It is mainly used for estimating the N-uptake in crops[29].
MCARI	$\frac{RE}{R} \times \{(RE - R) - 0.2\,(RE - G)\}$	It is mainly used for estimating the chlorophyll content[30].

Step 6: Then, using the pixel-by-value tool in Arc10.6, values for the geo-tagged points were extracted.

Output

Step 7: Pearson correlation analysis was done between the ground-truth SPAD value and the extracted VI value to find the best-fitting indices.

Step 8: Regression analysis was done to estimate the best-fitting regression equation and R^2 value between the ground-truth SPAD and extracted VI values.

Step 9: The best-fitting regression equation was further used to develop the predicted chlorophyll map for the study area.

Statistical analysis

Statistical analysis was done using Minitab software for validation. First, Pearson correlation analysis was done to identify the best VI having the highest correlation with ground-truth chlorophyll data. The correlation coefficient (R) is useful in determining the correlation strength between the two datasets. The mathematical formula for calculating the r-value is given in eq. (1). Next, the coefficient of determination (R^2) and root mean square error (RMSE) values were estimated to predict the model accuracy. Finally, regression (R^2) values were estimated for VIs (independent variable) and ground-truth chlorophyll data (dependent variable) to find the best line-of-fit. A higher R^2 and lower RMSE value indicate that the independent variable is highly predictable from the dependent variable. Therefore, eqs (2) and (3) were used to calculate R^2 and RMSE[17,18] respectively.

$$R = \frac{n\sum xy - (\sum x)(\sum y)}{\sqrt{n\sum(x^2) - (\sum x^2)}\sqrt{n\sum(y^2) - (\sum y^2)}}, \quad (1)$$

$$R^2 = \frac{\sum_{i=1}^{n}(y_i - x_i)^2}{\sum_{i=1}^{n}(y_i - \bar{y})^2}, \quad (2)$$

$$\text{RMSE} = \sqrt{\frac{\sum_{i=1}^{n}(x_i - y_i)^2}{n}}, \quad (3)$$

where x_i and y_i are the predicted and measured values respectively, $\bar{x}$ and $\bar{y}$ are the average predicted and measured values respectively, and n is the sample number.

Results and discussion

The UAV-collected high-resolution multispectral images for chlorophyll content yielded positive and strongly correlated results. The study area generated different VI maps, viz. NDVI, NDRE, GNDVI, REDVI, OSAVI and MCARI (Figure 4). Table 3 lists the mean values of different VIs. The map outcomes of VIs were different as each index uses various wavebands. These indices are useful for detecting differences in the greenness and chlorophyll content of crops. By utilizing the ground-data coordinates in ArcGIS 10.6, 15 points were selected from the indices map and extracted point values were using the pixel-by-value tool. Statistical analysis was done to establish a relationship between UAV-derived VI value and ground-truth chlorophyll data. Pearson correlation analysis helped identify the most sensitive VI with respect to the chlorophyll content. Figure 5 shows a positive and linear correlation between different VIs and ground-truth chlorophyll data.

Table 3 reveals that there is a difference between the VI values and SPAD readings. This is due to differences at the field level, as the research field consisted of different cotton varieties for experimental purposes. The SPAD readings ranged from 28.9 to 65.4. The range of values for different VIs was as follows: NDVI from 0.134 to 0.838, NDRE from 0.171 to 0.39, GNDVI from 0.264 to 0.648, REDVI from 0.009 to 0.05, OSAVI from 0.04 to 0.369, and MCARI from –0.002 to 0.137. The lowest and negative values in some indices show that they are sensitive to non-photosynthetic materials and background soil properties where the red edge values are higher than the NIR values in some parts of the pixel.

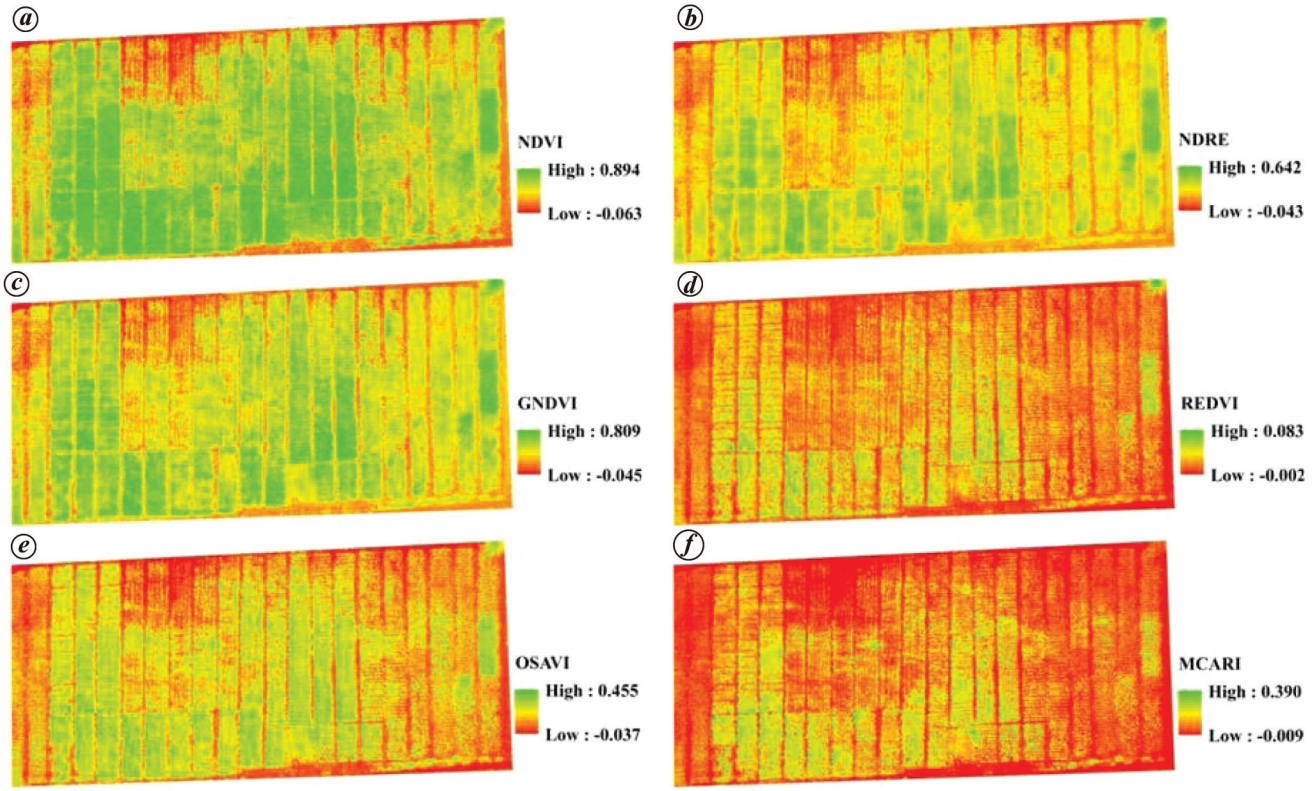

Figure 4. Vegetation index map generated using ArcGIS software: ***a***, NDVI; ***b***, NDRE; ***c***, GNDVI; ***d***, REDVI; ***e***, OSAVI; ***f***, MCARI.

Table 3. Ground truth SPAD value and vegetation index value for geo-tagged points

Latitude	Longitude	SPAD	NDVI	NDRE	GNDVI	REDVI	OSAVI	MCARI
11.0200	76.9297	35.5	0.319	0.228	0.395	0.015	0.104	0.004
11.0203	76.9306	38.2	0.366	0.325	0.430	0.011	0.070	0.001
11.0203	76.9297	35.1	0.134	0.171	0.264	0.009	0.040	–0.002
11.0199	76.9302	62.4	0.800	0.306	0.546	0.026	0.256	0.098
11.0202	76.9300	52.5	0.767	0.333	0.531	0.027	0.244	0.067
11.0199	76.9299	65.4	0.838	0.390	0.648	0.050	0.369	0.137
11.0200	76.9303	48.7	0.773	0.330	0.563	0.026	0.243	0.068
11.0201	76.9305	38.3	0.475	0.258	0.410	0.014	0.126	0.012
11.0199	76.9296	53.7	0.823	0.407	0.597	0.027	0.232	0.059
11.0202	76.9296	38.7	0.166	0.181	0.257	0.010	0.048	–0.001
11.0200	76.9293	50.1	0.723	0.290	0.544	0.031	0.280	0.080
11.0201	76.9299	28.9	0.471	0.246	0.361	0.013	0.122	0.012
11.0203	76.9304	45.5	0.588	0.228	0.419	0.020	0.205	0.043
11.0202	76.9294	39.4	0.351	0.233	0.324	0.011	0.084	0.004
11.0201	76.9295	51.6	0.745	0.312	0.521	0.021	0.205	0.053

Table 4 shows the regression equation and RMSE values for VIs. Among VIs, MCARI had a higher positive correlation coefficient ($R = 0.933$) with the ground chlorophyll data than the other indices. MCARI recorded values from 0.390 to –0.009 with R^2 value of 0.87 and RMSE of 3.91. This shows that MCARI has higher accuracy for predicting chlorophyll content. OSAVI recorded values from 0.455 to –0.037 with a higher positive correlation coefficient $R = 0.879$, R^2 value of 0.77 and RMSE of 5.19. REDVI had a positive correlation coefficient $R = 0.857$, and recorded values from 0.083 to –0.002 with R^2 value of 0.73 and RMSE of 5.60. A higher correlation coefficient indicates healthy/dense vegetation with more chlorophyll content, whereas lower values indicate stressed/sparse vegetation with low chlorophyll content.

The GNDVI values ranged from 0.809 to –0.045 with a positive correlation coefficient $R = 0.848$, R^2 value of 0.71 and RMSE of 5.77. On the other hand, a lower positive correlation coefficient ($R = 0.834$) was recorded with NDVI, having values from 0.894 to –0.063 with R^2 value of 0.69

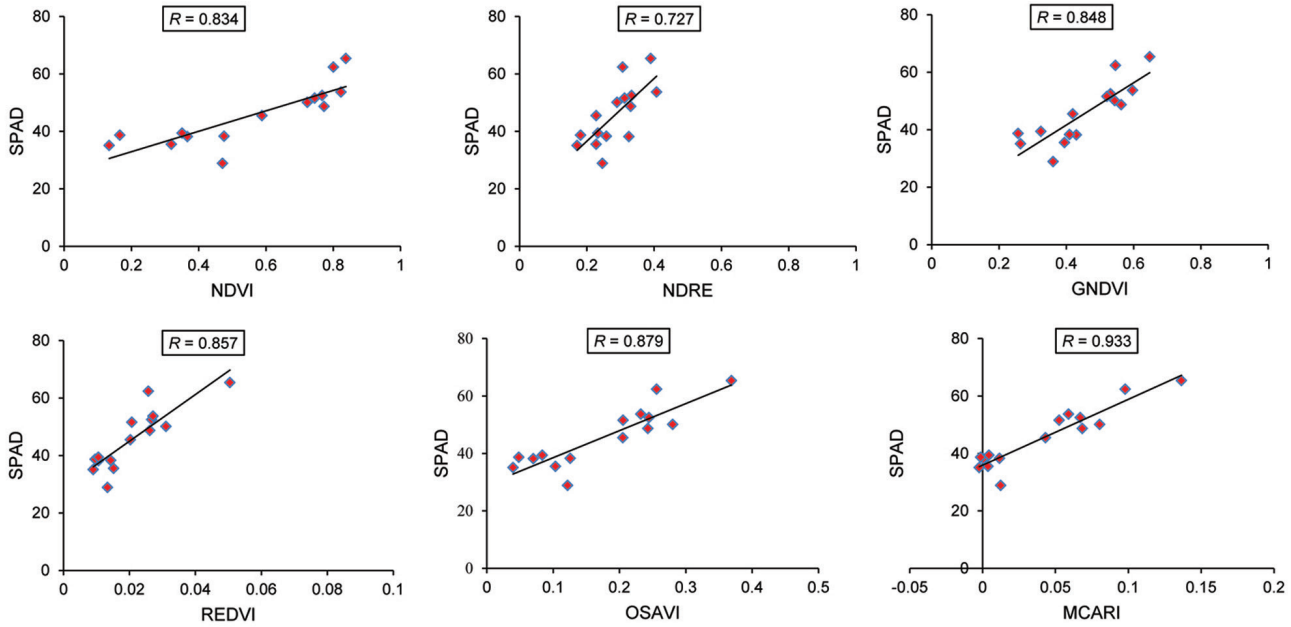

Figure 5. Relationship between NDVI, NDRE, GNDVI, REDVI, OSAVI, MCARI and SPAD chlorophyll readings using Pearson correlation analysis.

Table 4. Regression and RMSE analysis between NDVI, NDRE, GNDVI, REDVI, OSAVI, MCARI and SPAD value

	SPAD value		
Vegetation index	Regression equation	R^2	RMSE
NDVI	$y = 25.82 + 35.58x$	0.69	6.01
NDRE	$y = 14.78 + 109.1x$	0.52	7.47
GNDVI	$y = 12.25 + 73.5x$	0.71	5.77
REDVI	$y = 28.77 + 812x$	0.73	5.60
OSAVI	$y = 29.09 + 94.2x$	0.77	5.19
MCARI	$y = 35.91 + 229.3x$	0.87	3.91

and RMSE of 6.01. NDRE had the least positive correlation coefficient ($R = 0.727$) with values ranging from 0.642 to –0.043, and R^2 value of 0.52 and RMSE of 7.47.

Chlorophyll-sensitive VIs performed better than other indices using green and red wavelengths. These indices act as direct proxies to crop biochemistry[19], whereas the chlorophyll-sensitive indices act as indirect proxies. This is because the crop leaves are more translucent to red edge wavelength, which can penetrate more deeply into the leaf cells than red and blue wavelengths. Hence MCARI is significantly correlated to crop chlorophyll content than the other indices. This conforms with Raper and Varco[20] that chlorophyll-specific VIs are more suitable for predicting chlorophyll content.

Chlorophyll absorption showed a saturation tendency at lower chlorophyll content in the red region between 660 and 680 nm, thus weakening the sensitivity of VIs to increased chlorophyll content. Absorption in the region around 550 or 700 nm at increasing chlorophyll concentration also showed the same phenomenon[21]. As a result, spectral indices that include these bands in the later regions would be more precise in determining chlorophyll content[22].

The regression equation of the highly correlated vegetation index MCARI was further used to generate the chlorophyll map for the whole study area (Figure 6). The SPAD value ranged from 18.8 to 44.0. The regression equation was further tested for accuracy using the ground-truth SPAD data, resulting in an R^2 value of 0.79 (Figure 7). The higher chlorophyll status reveals the healthy condition of the crop, while the lower chlorophyll status depicts its stressed condition. These spatial variations can be further used for precise site-specific nitrogen management practices. They are also useful in discriminating the spatial chlorophyll content using the high-resolution multispectral imageries of UAVs at a regional scale.

Conclusion

Accurate, real-time and early identification of crop chlorophyll status is beneficial for agricultural management systems and assists in fertilizer application efficacy[23]. Chlorophyll concentration has been preferred by agronomists for growth diagnosis and is currently seeking to be predicted more accurately from spectral data. Chlorophyll content better depicts the interaction of matter and light per unit surface area[24]. Since chlorophyll accumulation is substantially correlated to crop biomass, VIs based on NIR bands could also be used to quantify chlorophyll accumulation at the canopy level. MCARI was best suited for assessing the chlorophyll content with a higher correlation coefficient

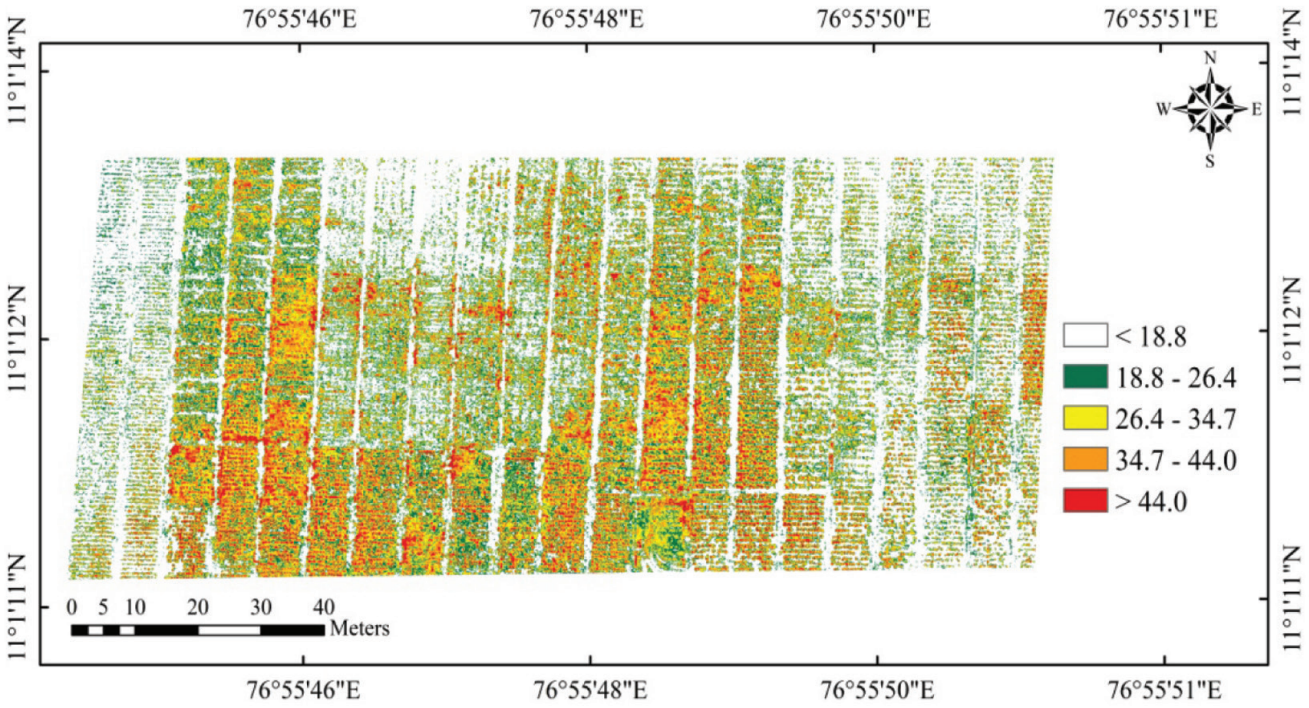

Figure 6. Chlorophyll map of the study area.

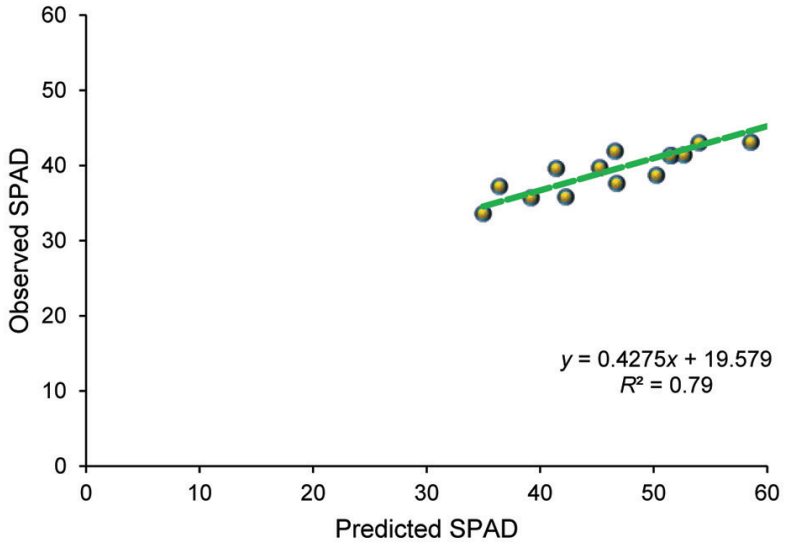

Figure 7. Accuracy assessment between observed and predicted SPAD values.

($R = 0.933$) and R^2 value of 0.87 among the VIs used in this study. MCARI is the only index that uses both red and red edge bands, as these regions are more specific for detecting vegetation status. This confirms that red edge-based VIs are more sensitive to chlorophyll content and perform better when compared to NDVI, as red edge light penetrates a leaf significantly more deeply than red or blue wavelengths. The chlorophyll map generated using the regression equation will be helpful in the farmers' decision-making for nutrient application.

1. Rani, A., Chaudhary, A., Nishant Sinha, K., Mohanty, M. and Chaudhary, R. S., Drone: the green technology for future agriculture. *Harit Dhara*, January–June 2019, **2**(1).
2. Tahir, M. N., Naqvi, S. Z. A., Lan, Y., Zhang, Y., Wang, Y., Afzal, M. and Amir, S., Real time estimation of chlorophyll content based on vegetation indices derived from multispectral UAV in the kinnow orchard. *Int. J. Precis. Agric. Aviat.*, 2018, **1**(1).
3. Boiarskii, B. and Hasegawa, H., Technologies of cartography and field monitoring using unmanned aerial vehicles (UAV). Actual problems of agroindustrial complex: a view of young researchers. Smolensk State Agricultural Academy, 2017, pp. 213–216.

4. Maddikunta, P. K. R., Hakak, S., Alazab, M., Bhattacharya, S., Gadekallu, T. R., Khan, W. Z. and Pham, Q. V., Unmanned aerial vehicles in smart agriculture: applications, requirements, and challenges. *IEEE Sensing J.*, 2021, **21**(16), 17608–17619.
5. Marang, I. J. *et al.*, Machine learning optimised hyperspectral remote sensing retrieves cotton nitrogen status. *Remote Sensing*, 2021, **13**, 1428; https://doi.org/10.3390/rs13081428.
6. Boiarskii, B. and Hasegawa, H., Comparison of NDVI and NDRE indices to detect differences in vegetation and chlorophyll content. *J. Mech. Continu. Math. Sci.*, 2019, **4**, 20–29.
7. De Castro, A. I., Shi, Y., Maja, J. M. and Peña, J. M., UAVs for vegetation monitoring: overview and recent scientific contributions. *Remote Sensing*, 2021, **13**, 2139.
8. Zhuo, W., Wu, N., Shi, R. and Wang, Z., UAV mapping of the chlorophyll content in a tidal flat wetland using a combination of spectral and frequency indices. *Remote Sensing*, 2022, **14**, 827.
9. Polonen, I., Hyperspectral imaging based biomass and nitrogen content estimations from light-weight UAV. *Proc. SPIE.*, 2013.
10. Wu, B., Meng, J., Li, Q., Yan, N., Du, X. and Zhang, M., Remote sensing-based global crop monitoring: experiences with China's CropWatch system. *Int. J. Digit. Earth*, 2014, **7**, 113–137.
11. Zheng, H. *et al*., Evaluation of RGB, color-infrared and multispectral images acquired from unmanned aerial systems for the estimation of nitrogen accumulation in rice. *Remote Sensing*, 2018, **10**, 824.
12. Shamshiri, R. R., Mahadi, M. R., Ahmad, D., Bejo, S. K., Aziz, S. A., Ismail, W. I. W. and Che Man, H., Controller design for an osprey drone to support precision agriculture research in oil palm plantations. In ASABE Annual International Meeting, Washington, USA, 2017, pp. 2–13.
13. Singh, K. D., Starnes, R., Kluepfel, D. A. and Nansen, C., Qualitative analysis of walnut trees rootstock using airborne remote sensing. In Sixth Annual Plant Science Symposium, UC Davis, CA, USA, 2017, p. 1.
14. Neupane, K. and Baysal-Gurel, F., Automatic identification and monitoring of plant diseases using unmanned aerial vehicles: a review. *Remote Sensing*, 2021, **13**, 3841; https://doi.org/10.3390/rs13193841.
15. Shaver, T. M., Kruger, G. R. and Rudnick, D. R., Crop canopy sensor orientation for late season nitrogen determination in corn. *J. Plant Nutr.*, 2017, **40**, 2217–2223.
16. Wu, Y., Li, W., Wang, Q. and Yan, S., Landslide susceptibility assessment using frequency ratio, statistical index and certainty factor models for the Gangu County, China. *Arab. J. Geosci.*, 2016, **9**(2), 84.
17. Gitelson, A. A. *et al.*, Relationship between gross primary production and chlorophyll content in crops: implications for the synoptic monitoring of vegetation productivity. *J. Geophys. Res. Atmos.*, 2006, 111.
18. Raper, T. and Varco, J., Canopy-scale wavelength and vegetative index sensitivities to cotton growth parameters and nitrogen status. *Precis. Agric.*, 2015, **16**, 62–76.
19. Sims, D. A. and Gamon, J. A., Relationships between leaf pigment content and spectral reflectance across a wide range of species, leaf structures and developmental stages. *Remote Sensing Environ.*, 2002, **81**, 337–354.
20. Xu, X., Gu, X., Song, X., Li, C. and Huang, W., Assessing rice chlorophyll content with vegetation indices from hyperspectral data. In International Conference on Computer and Computing Technologies in Agriculture, Springer, Berlin, Heidelberg, Germany, 2010, pp. 296–303.
21. Yao, X., Zhu, Y., Tian, Y., Feng, W. and Cao, W., Exploring hyperspectral bands and estimation indices for leaf nitrogen accumulation in wheat. *Int. J. Appl. Earth Obs. Geoinf.*, 2010, **12**, 89–100.
22. Xia, Y. *et al*., Using leaf dry matter to quantify the critical nitrogen dilution curve for winter wheat cultivated in eastern China. *Field Crops Res*., 2014, **159**, 33–42.
23. Zheng, H. *et al*., Evaluation of RGB, color-infrared and multispectral images acquired from unmanned aerial systems for the estimation of nitrogen accumulation in rice. *Remote Sensing*, 2018, **10**, 824.
24. Xie, Q. *et al*., Vegetation indices combining the red and red-edge spectral information for leaf area index retrieval. *IEEE J. Sel. Top. Appl. Earth Obs. Remote Sensing*, 2018, **11**, 1482–1493.
25. Amaral, L. R., Molin, J. P., Portz, G., Finazzi, F. B. and Cortinov, L., Comparison of crop canopy reflectance sensors used to identify sugarcane biomass and nitrogen status. *Precis. Agric.*, 2015, **16**, 15–28.
26. Shi, Y. *et al*., Unmanned aerial vehicles for high-throughput phenotyping and agronomic research. *PLoS ONE*, 2016, **11**(7), e0159781.
27. Lu, J., Miao, Y., Huang, Y., Shi, W., Hu, X., Wang, X. and Wan, J., Evaluating an unmanned aerial vehicle-based remote sensing system for estimation of rice nitrogen status. In Proceedings of the Fourth International Conference on Agro-Geoinformatics (Agro-geoinformatics), Istanbul, Turkey, 20 July 2015, pp. 198–203.
28. Shang, J. *et al.*, Mapping spatial variability of crop growth conditions using RapidEye data in Northern Ontario, Canada. *Remote Sensing Environ.*, 2015, **168**, 113–125.
29. Pandit, S., Tsuyuki, S. and Dube, T., Landscape-scale aboveground biomass estimation in buffer zone community forests of Central Nepal: coupling *in situ* measurements with Landsat 8 satellite data. *Remote Sensing*, 2018, **10**, 1–18.
30. Li, M. *et al*., Temporal variability of precipitation and biomass of alpine grasslands on the Northern Tibetan Plateau. *Remote Sensing*, 2019, **11**, 360.

ACKNOWLEDGEMENT. We thank the Department of Remote Sensing and GIS, Tamil Nadu Agricultural University, Coimbatore for technical assistance while conducting this study.

Received 28 June 2022; revised accepted 7 September 2022

doi: 10.18520/cs/v123/i12/1473-1480